frontiers | Frontiers in Physics

TYPE Original Research
PUBLISHED 30 May 2023
DOI 10.3389/fphy.2023.1188608

OPEN ACCESS

EDITED BY
Baole Lu,
Northwest University, China

REVIEWED BY
Xiaohui Li,
Shaanxi Normal University, China
Zhenxu Bai,
Hebei University of Technology, China
Muhammad Hafiz Abu Bakar,
Putra Malaysia University, Malaysia

*CORRESPONDENCE
Fengping Yan,
fpyan@bjtu.edu.cn

RECEIVED 17 March 2023
ACCEPTED 09 May 2023
PUBLISHED 30 May 2023

CITATION
Wang X, Yan F, Guo H, Wang W, Qin Q, Yang D, Wang P, Li T, Yu C, Guan B, Kumamoto K, Suo Y and Bai Y (2023), Single longitudinal mode narrow linewidth thulium-doped fiber laser based on an eye-shaped dual-ring filter. *Front. Phys.* 11:1188608. doi: 10.3389/fphy.2023.1188608

Single longitudinal mode narrow linewidth thulium-doped fiber laser based on an eye-shaped dual-ring filter

Xiangdong Wang[1], Fengping Yan[1]*, Hao Guo[1], Wei Wang[2], Qi Qin[1], Dandan Yang[1], Pengfei Wang[1], Ting Li[1], Chenhao Yu[1], Biao Guan[1], Kazuo Kumamoto[3], Yuping Suo[4] and Yan Bai[5]

[1]School of Electronic and Information Engineering, Beijing Jiaotong University, Beijing, China, [2]Key Laboratory of Luminescence and Optical Information, Ministry of Education, School of Physical Science and Engineering, Institute of Optical Information, Beijing Jiaotong University, Beijing, China, [3]Department of Electronics, Information, and Communication Engineering, Osaka Institute of Technology, Osaka, Japan, [4]Department of Gynecology and Obstetrics, The Fifth Clinical Medical College of Shanxi Medical University, Taiyuan, China, [5]College of Electrical Engineering, Hebei University of Architecture, Zhangjiakou, Hebei, China

A single-longitudinal-mode (SLM) thulium-doped fiber laser, based on an eye-shaped passive dual-ring filter, is designed and constructed. The eye-shaped passive compound cavity consisting of four couplers is used to increase the longitudinal mode spacing, and its performance is numerically analyzed in detail. A homemade uniform fiber Bragg grating serves as a wavelength selection device and a saturable absorber is used to further suppress the intense longitudinal mode competition in the laser cavity, ensuring the single-longitudinal-mode output. The experimental results demonstrate a laser output with a center wavelength of 2,049.85 nm and an optical signal-to-noise ratio of 63 dB. Moreover, the power fluctuation is less than 0.6 dB, and the center wavelength fluctuation is less than 0.03 nm over a continuous measurement period of 60 min, demonstrating an excellent stability. The laser linewidth is measured using an unbalanced Michelson interferometer and β-separation line method, resulting in a linewidth of 11.22 kHz.

KEYWORDS

single longitudinal mode, thulium-doped fiber laser, high power, narrow linewidth, 2 μm

1 Introduction

Currently, fiber lasers have been applied in a wide range of fields, such as spectroscopy, monitoring Material characteristic testing, optical sensor, high-resolution nonlinear microscopy imaging, etc., due to their compact structure, low cost, good beam quality, and no need for calibration [1–3]. And different monitoring methods have been used to observe the beam characteristics [4–6], In particular, Thulium-doped fiber laser (TDFL) working around the 2.0 μm band can induce a relatively low harm to the human eyes. The reason lies in that when reaching the human eyes, the 2.0 μm laser will be strongly absorbed by the cornea and crystalline lens inside the eye, making it difficult to reach the highly sensitive retina [7, 8]. Moreover, the 2.0 μm band laser features a very weak penetration ability in the biological tissues, and the penetration depth is only about 500 μm. Hence, using a 2.0 μm band laser for medical surgery can accelerate the blood coagulation and reduce the surgical trauma. In addition, TDFLs are widely used in ophthalmic surgery, dental surgery, and surface disease treatment. In recent years, TDFL has also achieved good therapeutic effects in urinary system symptoms, such as prostate hyperplasia, bladder tumors, and the ureteral strictures [9]. Meanwhile, the 2.0 μm band laser also appears in industrial cutting and welding, atmospheric detection of toxic gas (CO, N_2O, CH_4), military wind and radar detection, differential absorption radar, portable laser ranging, as well as in other scientific fields [10–15]. However, the thulium-doped fiber (TDF) characterizes a relatively low gain around 2,050 nm, making it challenging to construct a single-longitudinal-mode (SLM) TDFL in this wavelength range.

In 2004, [16] fabricated a distributed-feedback single-frequency TDFL with a cavity length of only 5 cm, pumped by a 793 nm Ti: sapphire laser, and the laser central wavelength was 1735 nm. In 2007, [17] achieved a single-frequency TDFL with an output power of 20 W and an output laser wavelength of 1.93 μm. In 2013, [18] developed a 1.95 μm single-frequency TDFL with a maximum output power of 200 mW and an optical signal-to-noise ratio (OSNR) of higher than 68 dB. In 2019, [19] realized a four-wavelength switchable single-frequency fiber laser with an OSNR greater than 80 dB and linewidth less than 700 Hz.

Currently, most of the proposed SLM lasers working in 2,050 nm band [20–22] use thulium-holmium co-doped fiber as the gain fiber and feature short laser cavity structures. However, the short laser cavity structure is limited by the quenching efficiency, and the maximum gain factor is less than 2 dB/cm. Thus, it is difficult to increase the output power by use of a short laser cavity structures, which also may cause a serious spatial hole burning effect. Using a ring cavity to increase the length of the TDFL in order to provide enough gain is a good alternative. The long ring cavity can effectively increase the output power, and a traveling wave ring cavity can effectively suppress the spatial hole burning. On the other hand, narrowband filters can be added in the laser cavity to achieve narrow linewidth output, which has been extensively reported in the C-band [23–25]. Furthermore, by adding an unpumped active fiber into the main cavity or Use of three-dimensional materials to act as a saturable absorber (SA) and using the dynamic self-tracking narrowband grating formed by the standing wave saturation effect [26], the suppression of multiple longitudinal modes can be achieved [27, 28]. However, using a single SA requires a sufficiently long fiber to meet the requirement, leading to a lower slope efficiency. It is worthing noting that the SLM lasers feature compound cavity structures can be used to achieve suppression of multiple longitudinal modes with simple configurations. The multi-ring compound cavities usually consist of a main cavity that provides gain and one or several passive sub-ring cavities, each of which is composed of one or more optical fiber couplers [19, 29–31]. The advantages of the compound cavity structures are low cost and high flexibility. By optimizing the length of each sub-ring cavity and the coupling ratio of the couplers, an ideal filtering effect can be achieved, making it a relatively ideal filtering component to construct 2.0 μm SLM fiber lasers.

This paper adopts a compound ring cavity structure and utilizes a home-made uniform fiber Bragg grating (UFBG) to achieve wavelength selection. Combining a new type of quad-coupler double ring compound cavity (QCDR-CC) with a narrowband self-tracking narrowband grating based on unpumped TDF, a SLM output is realized. Firstly, the design thinking and performance of the QCDR-CC are theoretically analyzed and experimentally verified in detail. The SLM operation is confirmed and evaluated by integrating the QCDR-CC and SA in the laser cavity. Subsequently, the wavelength and power fluctuations of the laser as well as the stability of the SLM output are demonstrated for more than 60 min. Finally, the linewidth of the SLM is measured using the linewidth system.

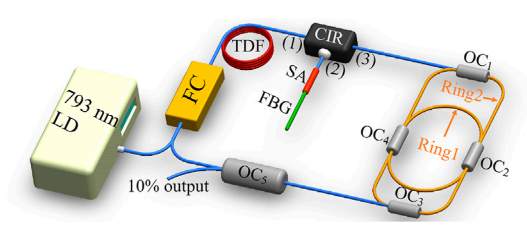

FIGURE 1
Schematic diagram of a SLM TDFL structure. The abbreviations employed in the Figure are: thulium-doped fiber (TDF); fiber combiner (FC); fiber circulator (CIR); optical fiber coupler (OC); saturable absorber (SA).

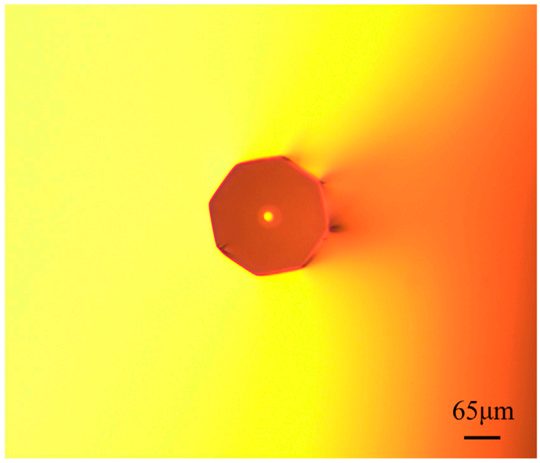

FIGURE 2
Cross-sectional view of the double-clad thulium-doped fiber.

2 Experimental setup and principle

2.1 Experimental setup

The schematic diagram of the proposed structure of the SLM TDFL is shown in Figure 1. A 793 nm semiconductor laser with a maximum output power of 12 W was used as the pump source and injected into the ring cavity through a beam combiner. The gain medium was a double-clad TDF (Nufern, SM-TDF-10P/130-M) featuring a core/cladding diameter of 10/130 μm, a numerical aperture of 0.15, and a length of 5 m. The absorption coefficient of TDF in 793 nm is 4.5 dB/m, which provides a sufficient gain for the laser. Figure 2 shows a cross-section of the double-clad thulium-

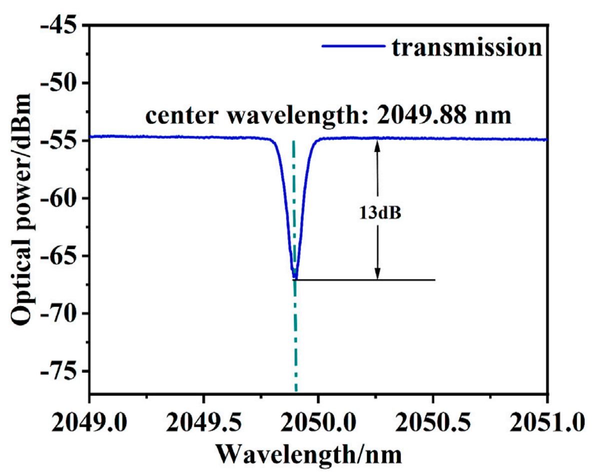

FIGURE 3
Reflection spectrum of the UFBG.

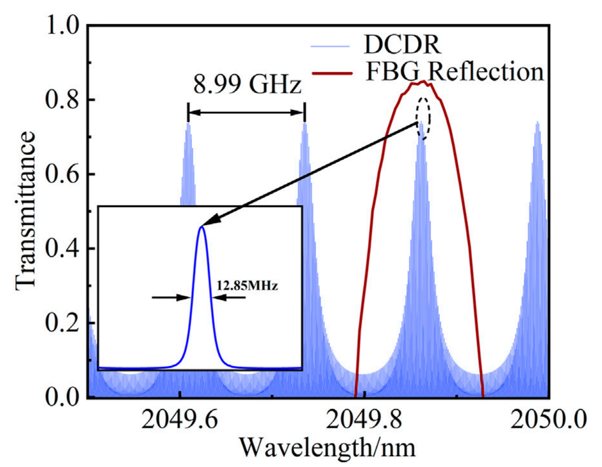

FIGURE 4
Transmission spectrum of the eye-shaped passive sub-cavity and the reflection spectrum of the UFBG.

doped fiber measured by an optical microscope, which features an octagonal shape to improve the pump absorption efficiency.

As shown in Figure 1, one of the ends of the doped fiber is connected to the 1-port of the ring resonator, which allows the laser to run unidirectionally. The 2-port of the ring resonator is fused with an unpumped TDF to form a SA, followed by a home-made UFBG as a narrowband high reflector. The UFBG was written by the phase mask method using a 248 nm KrF excimer laser, with a mask period of 1,423.7 nm and a length of 2 cm. The transmission spectrum of the UFBG were measured using a Yokogawa AQ6375B optical spectrum analyzer (OSA) with a resolution of 0.05 nm, as shown in Figure 3. The transmission depth of the UFBG was 13 dB, corresponding to a reflectivity of 93.69%. The 3 dB bandwidth of the UFBG reflection peak was 0.071 nm, corresponding to a spectral range of approximately 5.07 GHz. The laser signal, reflected by the UFBG, passed through the SA and then underwent a SLM selection in the eye-shaped passive compound cavity. A 1 × 2 optical fiber coupler was used to output 10% of the laser from the cavity. Finally, the total cavity length of the laser was approximately 21.79 m, corresponding to a longitudinal mode spacing of approximately 9.5 MHz.

2.2 SLM implementation principle

The 3 dB bandwidth of the UFBG reflection spectrum is 0.071 nm, corresponding to a spectral range of approximately 5.07 GHz in the 2,050 nm band. The longitudinal mode spacing of the constructed ring cavity is about 9.5 MHz. The proposed eye-shaped passive compound cavity filters out one longitudinal mode within the FBG bandwidth from about 533 existent longitudinal modes. Moreover, the mode is capable of oscillating in the main cavity to achieve a SLM operation. In order to achieve this goal, the following conditions should be met:

1) the effective free spectral range (FSR) of the compound cavity should be greater than half of the FBG reflection bandwidth in order to ensure that only one effective transmission band is present;
2) the bandwidth of the effective transmission band of the compound cavity should be twice the main cavity longitudinal mode spacing [31].

Herein, the structure of the eye-shaped compound cavity, as presented in Figure 1, is composed of four 2 × 2 optical fiber couplers. The coupling ratio of OC_1 and OC_3 is 50:50, while that of OC_2 and OC_4 is 2:98. Moreover, $Ring_1$, with a length of 3.0 m, is constructed by OC_2 and OC_4, while $Ring_2$, with a length of 3.033 m, is built by OC_1 and OC_3. According to FSR = $c/(n*L)$, where c is the speed of light (3×10^8 m/s), n is the refractive index of the fiber core (1.447) and L is the cavity length, the FSR of $Ring_1$ is about 68.4 MHz, and that of $Ring_2$ is about 69.1 MHz. According to Vernier effect, the effective FSR of the compound cavity should be the least common multiple of the FSRs of both rings, which is about 4.7 GHz. In the 2,050 nm band, the corresponding wavelength range is approximately 0.064 nm, which is comparable to the reflection bandwidth of the FBG. Based on these findings, further longitudinal mode selection of the laser is performed. The 3 dB bandwidth of the main resonance peak of the compound cavity filter is determined by the length of the longest ring in the sub-cavity. The longer the ring length is, the narrower the bandwidth it will be. The bandwidth of the interference peak of the compound cavity can be obtained referring to the below equation [30, 32]:

$$\Delta v = \frac{c\delta}{2\pi n_{eff} L_1}$$

where L_1 represents the length of the main ring of the compound cavity and δ indicates the loss of light after one round trip in the compound cavity. It can be expressed as follows:

$$\delta = \ln\left(\frac{I_o}{I_i}\right)$$

Here, I_o represents the input intensity of light whereas I_i represents the remaining intensity of light after one round of

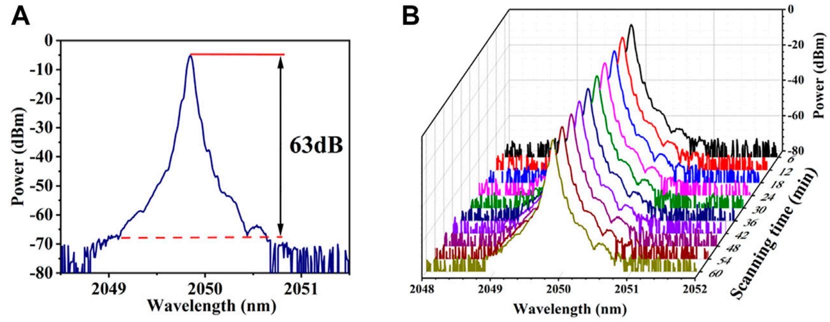

FIGURE 5
(A) Laser output spectrum and **(B)** ten consecutive scans at 6 min interval.

transmission in the compound cavity. Given that the insertion losses of the four couplers are similar and equal to 0.2 dB, the narrowband interference peak bandwidth is equal to 12.5 MHz, which is approximately 1.45 times the longitudinal mode spacing of the main cavity. This ensures that there is only one longitudinal mode output in the passive eye-shaped compound cavity effective transmission passband.

Also, the proposed passive eye-shaped compound cavity filter was simulated and the simulation method is consistent with the previous work [33]. The simulation results are shown in Figure 4 where the red line represents the normalized reflection spectrum of the UFBG. The FSR of the compound cavity is equal to 0.13 nm (~8.99 GHz), which is slightly different from the estimated value. However, the FSR obtained from the simulation still satisfies the required condition as it is greater than 0.5 times and less than twice the FBG reflection bandwidth, which ensures that there is only one dominant transmission band within the FBG reflection bandwidth. Furthermore, the inset in Figure 4 shows a partial enlargement of the transmission spectrum of the simulated eye-shaped compound cavity filter. The interference-formed transmission peak in the filter has a 3 dB bandwidth of around 12.85 MHz, which is essentially not far from the previously specified 12.5 MHz. At the same time, the simulation shows that the ratio of the main peak to the side lobe is 0.74 and 0.71, respectively, indicating that the gain competition is relatively intense. To handle these problems, the SA is introduced to suppress mode competition and form a narrower bandwidth filter to suppress side lobes. The proposed eye-shaped compound cavity combining with the SA ensures the SLM operation of the laser.

3 Experimental results and analysis

The laser configuration was built and tested under room temperature, and it was placed on an optical platform and isolated from the pump source. The entire laser system was not equipped with any temperature or isolation devices. Also, the laser threshold was 2.6 W, and a stable output was achieved by increasing the pump power to 3.3 W. The spectrum, measured by the connected OSA, is shown in Figure 5 as well and the OSA resolution was set to 0.05 nm. The center wavelength of the laser was 2,049.85 nm, which was offset by 0.03 nm compared to the center wavelength of the FBG transmission peak. This wavelength drift was caused by the temperature and the stress disturbances caused by fixing the UFBG during the measurement. Referring to Figure 5A, it can be seen that the OSNR of the output laser is equal to 60 dB. Furthermore, the output spectrum of the laser was scanned every 6 min, and the spectra obtained from ten consecutive scans is shown in Figure 5B. The center wavelength and the peak power of the laser output spectrum did not fluctuate significantly during the observation time, indicating that the laser discloses a good stability at room temperature. In order to further study the output stability of the laser, a continuous scanning of the center wavelength and the output power was performed, as shown in Figure 6. The fluctuation range of the center wavelength was just 0.03 nm, which is smaller than the minimum resolution of the spectrometer of 0.05 nm, and the output power fluctuation was limited to 0.58 dB.

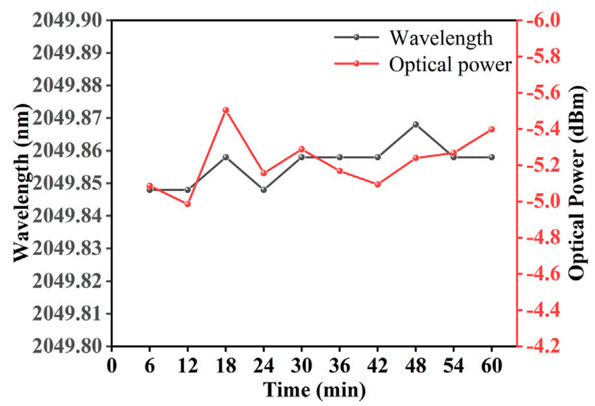

FIGURE 6
Fluctuation of laser center wavelength and output power.

The self-homodyne method was used to measure the SLM property of the output laser. The output end of the laser was connected to a 12.5 GHz photodetector (PD) module to convert the optical signal to electrical signal. The converted electrical signal was then sent to a signal analyzer. In theory, when only one laser longitudinal mode appears in the output signal, only the zero frequency can be observed in the signal analyzer. However, when two or more laser longitudinal modes are sent to the output signal,

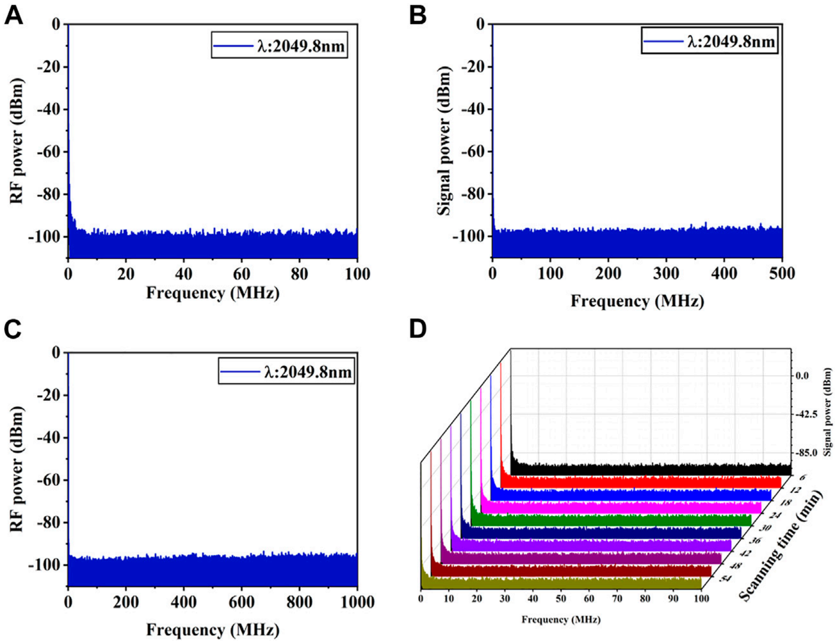

FIGURE 7
Self-homodyne results with the presence of sub-cavity and SA **(A)** for the frequency range of 0–100 MHZ, **(B)** for the frequency range of 0–500 MHz, **(C)** for the frequency of 0–1 GHz, and **(D)** for the frequency of 0–1 GHz measured at 6 min intervals.

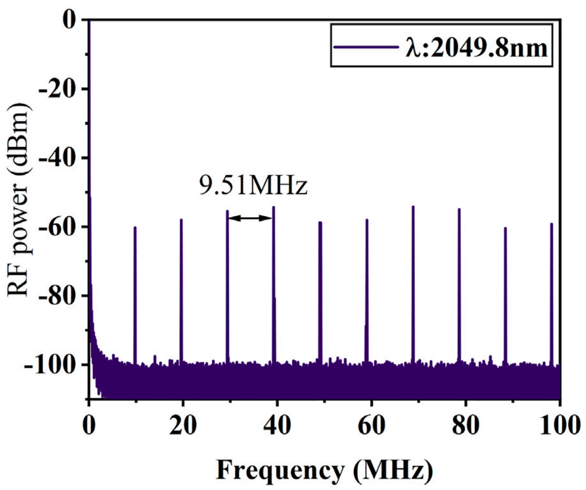

FIGURE 8
Spectrum without SA and passive compound sub-cavity.

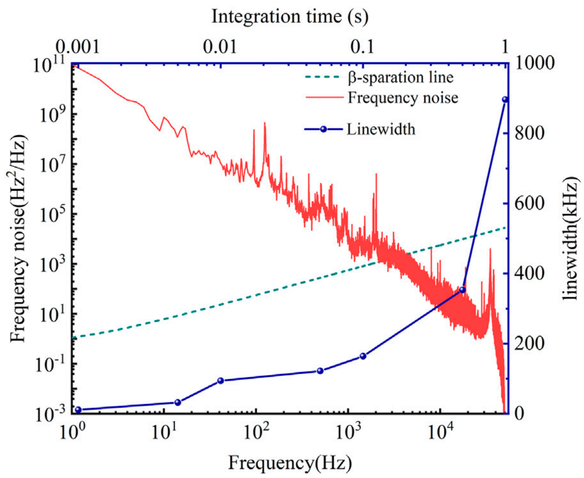

FIGURE 9
Frequency noise power spectral density and linewidth of the laser.

the signal analyzer will display the beat frequencies at non-zero frequencies. The laser beat frequency results, with scanning ranges of 100 MHz, 500 MHz, and 1 GHz, are displayed in Figure 7. It can be seen from Figure 7 that there is no beat frequency signal within the scanning range. Figure 8 shows the spectrum without the use of an SA and a passive compound cavity for reference. The obvious non-zero longitudinal mode frequency peaks can be observed, indicating that the laser is in a multi-longitudinal mode operation state. Therefore, it can be concluded that the un-pumped TDF and the passive cavity play a decisive role in the formation of a SLM mode operation of the laser.

The phase noise demodulation method and the linewidth measurement system composed of a 3 × 3 coupler and 2 F rotation mirrors (FRMs) are used to obtain the linewidth of the output wavelength. Compared to the traditional delay self-heterodyne linewidth measurement method by use of an ultralong delay line, the use of a 50 m long SMF as a delay line can reduce losses. Both FRM reflected lights demonstrate a time difference due to different transmission distances and then they are received by two identical PDs. The output signals from PDs are collected by a data acquisition board to calculate the power spectral density (PSD) of the instantaneous phase and frequency fluctuations of the laser. The linewidth, obtained by this linewidth measurement method, widens with the measurement time as a result of *1/f* noise in the power spectral density of the frequency fluctuations. It is important to mention that the measurement was carried out in a relatively quiet environment. The frequency noise spectrum of the laser was calculated and plotted in Figure 9. It can be clearly seen that the linewidth broadens with the increase of measurement time. For instance, the linewidth at the minimum measurement time (0.001 s) is 11.2 kHz, whereas, at the longest measurement time (1 s), it is approximatively equal to 896 kHz.

4 Conclusion

This paper demonstrates a SLM TDFL based on an eye-shaped QCDR-CC and SA. At room temperature, the proposed fiber laser achieved a stable laser output with a central wavelength of 2,049.85 nm and an OSNR of 60 dB. Over a continuous measurement period of 60 min, the maximum power fluctuation of the laser output was lower than 0.6 dB, and the wavelength fluctuation of the central wavelength was less than the minimum resolution of the OSA (equal to 0.05 nm). Therefore, the laser output features a good stability. Finally, the SLM operation characteristic of the laser was verified using the self-homodyne method, and the laser linewidth was measured to be 11.22 kHz based on frequency noise analysis. The presented results are quite attractive. A wealth of applications could be carried out based on the proposed TDFL, like Lidar and free-space optical communication systems.

A SLM TDFL based on an eye-shaped QCDR-CC and SA was proposed with a central wavelength of 2,049.85 nm and an OSNR of 60 dB. The measured linewidth was 11.22 kHz under a measurement time of 0.01 s. The proposed TDFL is of vital importance of fiber sensor and communication applications.

Data availability statement

The original contributions presented in the study are included in the article/Supplementary Material, further inquiries can be directed to the corresponding author.

Author contributions

XW: Writing—original draft. FY: conceptualization. HG and TL: validation. QQ and DY: Resources; PW, CY, and KK: data curation; YS and YB: writing—original draft preparation. All authors contributed to the article and approved the submitted version.

Funding

This work was supported by the National Natural Science Foundation of China (Nos. 61827818, 61975105, 61975009, 61975049, 2021050, and 62005013).

Acknowledgments

The authors would like to thank the editors and reviewers for their efforts in supporting the publication of this paper.

Conflict of interest

The authors declare that the research was conducted in the absence of any commercial or financial relationships that could be construed as a potential conflict of interest.

Publisher's note

All claims expressed in this article are solely those of the authors and do not necessarily represent those of their affiliated organizations, or those of the publisher, the editors and the reviewers. Any product that may be evaluated in this article, or claim that may be made by its manufacturer, is not guaranteed or endorsed by the publisher.

References

1. Zhang Z, Zhang J, Chen Y, Xia T, Wang L, Han B, et al. *Bessel terahertz pulses from superluminal laser plasma filaments* (2022).

2. Guan M, Chen D, Hu S, Zhao H, You P, Meng SJUS, *Theoretical insights into ultrafast dynamics in quantum materials* (2022). 2022.

3. Li X, Huang X, Hu X, Guo X, Han YJO, Technology L, Recent progress on mid-infrared pulsed fiber lasers and the applications. *Recent Prog mid-infrared pulsed fiber lasers Appl* (2023) 158:108898. doi:10.1016/j.optlastec.2022.108898

4. Liu X, Pang MJL, Reviews P, Revealing the buildup dynamics of harmonic mode-locking states in ultrafast lasers. *Revealing buildup Dyn harmonic mode-locking States ultrafast lasers* (2019) 13:1800333. doi:10.1002/lpor.201800333

5. Liu X, Popa D, Akhmediev NJPr.l., Revealing the transition dynamics from. *Q Switching Mode Locking A Soliton Laser* (2019) 123:093901. doi:10.1103/physrevlett.123.093901

6. Liu X, Yao X, Cui YJPr.l., Real-time observation of the buildup of soliton molecules, 121 (2018) 023905.

7. Kim W, Bowman SR, Baker C, Villalobos G, Shaw B, Sadowski B, et al. Holmium-doped laser materials for eye-safe solid state laser application. In: *Laser Technology for defense and security X*. Washington: SPIE (2014). p. 9–14.

8. Scholle K, Lamrini S, Koopmann P, Fuhrberg P, 2 μm laser sources and their possible applications. In: *Frontiers in guided wave optics and optoelectronics*. London: IntechOpen (2010).

9. Abad PG, Del Peso AC, Arjona MF, Holmium: YAG laser ablation of upper urinary tract transitional cell carcinoma with new olympus digital flexible ureteroscope. *Urol Ann* (2013) 5:212–4. doi:10.4103/0974-7796.115748

10. Andreev S, Mironchuk E, Nikolaev I, Ochkin V, Spiridonov M, Tskhai S, High precision measurements of the 13 CO 2/12 CO 2 isotope ratio at atmospheric pressure in human breath using a 2 μm diode laser. *Appl Phys B* (2011) 104:73–9. doi:10.1007/s00340-011-4602-4

11. Niwa Massaki ABM, Eimpunth S, Fabi SG, Guiha I, Groff W, Fitzpatrick R, Treatment of melasma with the 1,927-nm fractional thulium fiber laser: A retrospective

analysis of 20 cases with long-term follow-up. *Lasers Surg Med* (2013) 45:95–101. doi:10.1002/lsm.22100

12. Voo N, Sahu J, Ibsen M, 345-mW 1836-nm single-frequency DFB fiber laser MOPA. *IEEE Photon Tech Lett* (2005) 17:2550–2. doi:10.1109/lpt.2005.859401

13. De Young RJ, Barnes NP, Profiling atmospheric water vapor using a fiber laser lidar system. *Appl Opt* (2010) 49:562–7. doi:10.1364/ao.49.000562

14. Li J, Sun Z, Luo H, Yan Z, Zhou K, Liu Y, et al. Wide wavelength selectable all-fiber thulium doped fiber laser between 1925 nm and 2200 nm. *Opt express* (2014) 22:5387–99. doi:10.1364/oe.22.005387

15. Ma W, Wang T, Su Y, Zhang Y, Liu P, Jia Q, et al. Wavelength-spacing switchable dual-wavelength single longitudinal mode thulium-doped fiber laser at 1.9 μm. *IEEE Photon J* (2016) 8:1–8. doi:10.1109/jphot.2016.2616515

16. Agger S, Povlsen JH, Varming P, Single-frequency thulium-doped distributed-feedback fiber laser. *Opt Lett* (2004) 29:1503–5. doi:10.1364/ol.29.001503

17. Gapontsev D, Platonov N, Meleshkevich M, Mishechkin O, Shkurikhin O, Agger S, et al. 20W single-frequency fiber laser operating at 1.93 um. In: Conference on Lasers and Electro-Optics. Baltimore: Optical Society of America (2007). p. CFI5.

18. He X, Xu S, Li C, Yang C, Yang Q, Mo S, et al. 195 μm kHz-linewidth single-frequency fiber laser using self-developed heavily Tm̃3+-doped germanate glass fiber. *Opt express* (2013) 21:20800–5. doi:10.1364/oe.21.020800

19. Feng T, Jiang M, Wei D, Zhang L, Yan F, Wu S, et al. Four-wavelength-switchable SLM fiber laser with sub-kHz linewidth using superimposed high-birefringence FBG and dual-coupler ring based compound-cavity filter. *Opt express* (2019) 27:36662–79. doi:10.1364/oe.27.036662

20. Wu J, Yao Z, Zong J, Chavez-Pirson A, Peyghambarian N, Yu J, Single-frequency fiber laser at 2.05 um based on ho-doped germanate glass fiber. In: *Fiber lasers VI: Technology, systems, and applications*. Washington: SPIE (2009). p. 358–64.

21. Geng J, Wang Q, Luo T, Case B, Jiang S, Amzajerdian F, et al. Single-frequency gain-switched Ho-doped fiber laser. *Opt Lett* (2012) 37:3795–7. doi:10.1364/ol.37.003795

22. Li L, Zhang B, Yin K, Hou J, 75 W single-frequency, thulium-doped fiber laser at 2.05 μm. *Laser Phys Lett* (2015) 12:095103. doi:10.1088/1612-2011/12/9/095103

23. Cheng X, Shum P, Tse C, Zhou J, Tang M, Tan W, et al. Single-longitudinal-mode erbium-doped fiber ring laser based on high finesse fiber Bragg grating Fabry–Pérot etalon. *IEEE Photon Tech Lett* (2008) 20:976–8. doi:10.1109/lpt.2008.922974

24. Sun T, Guo Y, Wang T, Huo J, Zhang L, Widely tunable wavelength spacing dual-wavelength single longitudinal mode erbium doped fiber laser. *Opt Fiber Tech* (2014) 20:235–8. doi:10.1016/j.yofte.2014.02.006

25. Yeh C-H, Chow C-W, Chen K-H, Chen J-H, Employing dual-saturable-absorber-based filter for stable and tunable erbium-doped fiber ring laser in single-frequency. *Laser Phys* (2011) 21:924–7. doi:10.1134/s1054660x11090271

26. Li X, Huang X, Han Y, Chen E, Guo P, Zhang W, et al. High-performance γ-MnO2 dual-core. *Pair-Hole Fiber Ultrafast Photon* (2023) 3:0006.

27. Feng S, Lu S, Peng W, Li Q, Feng T, Jian S, Tunable single-polarization single-longitudinal-mode erbium-doped fiber ring laser employing a CMFBG filter and saturable absorber. *Opt Laser Tech* (2013) 47:102–6. doi:10.1016/j.optlastec.2012.08.020

28. Xu P, Hu Z, Ma M, Jiang N, Hu Y, Mapping the optical frequency stability of the single-longitudinal-mode erbium-doped fiber ring lasers with saturable absorber. *Opt Laser Tech* (2013) 49:337–42. doi:10.1016/j.optlastec.2012.09.030

29. Feng S, Mao Q, Tian Y, Ma Y, Li W, Wei L, Widely tunable single longitudinal mode fiber laser with cascaded fiber-ring secondary cavity. *IEEE Photon Tech Lett* (2013) 25:323–6. doi:10.1109/lpt.2012.2235141

30. Feng T, Ding D, Zhao Z, Su H, Yan F, Yao XS, Switchable 10 nm-spaced dual-wavelength SLM fiber laser with sub-kHz linewidth and high OSNR using a novel multiple-ring configuration. *Laser Phys Lett* (2016) 13:105104. doi:10.1088/1612-2011/13/10/105104

31. Feng T, Wei D, Bi W, Sun W, Wu S, Jiang M, et al. Wavelength-switchable ultra-narrow linewidth fiber laser enabled by a figure-8 compound-ring-cavity filter and a polarization-managed four-channel filter. *Opt Express* (2021) 29:31179–200. doi:10.1364/oe.439732

32. Feng T, Ding D, Yan F, Zhao Z, Su H, Yao XS, Widely tunable single-/dual-wavelength fiber lasers with ultra-narrow linewidth and high OSNR using high quality passive subring cavity and novel tuning method. *Opt Express* (2016) 24:19760–8. doi:10.1364/oe.24.019760

33. Yang D, Yan F, Feng T, Qin Q, Li T, Yu C, et al. Stable narrow-linewidth single-longitudinal-mode thulium-doped fiber laser by exploiting double-coupler-based double-ring filter. *Infrared Phys Tech* (2023) 129:104568. doi:10.1016/j.infrared.2023.104568